Supporting Information for:

Assembly of RNA nanostructures on supported lipid bilayers

Aleksandra Dabkowska, Agnes Michanek, Luc Jaeger, Michael Rabe, Arkadiusz Chworos, Fredrik Höök, Tommy Nylander and Emma Sparr

A. Supplementary Tables

Table S1: Sequences of tRNA units used in this study. Nomenclature: A, B, C and D indicate the type of the unit: they are represented in a clock-wise fashion with respect of their KL motifs within the context of the tRNA tectosquare (TS). 3' tails are numbered as 1t and 1t', 1t being complementary to 1t'. Tails can form triple base pairs. This is specified by a small t after their number. Color code: yellow=KL, Blue= 3'-tail, green= major triple helix interaction.
TS3 is formed of A1t, B1t, C1t and D1t; TS4 is formed of A1t', B1t', C1t' and D1t'; TO3-4 is formed of the assembly of TS3 with TS4.

TS3	A1t	GGCAGCCUCCGUGGUUCGAAUCCACGUACCAGCCUGGAUG**AAGUGGACA**CGUCCAGGCUGGUAU
		GGCCGAGCGGCUGAAGGCACUCGUAGUG**AAGGAGGCA**CGCUACGAGUAGGUUGCC**CCAGAG**UC
	B1t	GGCAGCCUCCGUGGUUCGAAUCCACGUACCAGCCUGGAUG**AAGCCUGCA**CGUCCAGGCUGGUAU
		GGCCGAGCGGCUGAAGGCACUCGUAGUG**AAGUCCAGA**CGCUACGAGUAGGUUGCC**CCAGAG**UC
	C1t	GGCAGCCUCCGUGGUUCGAAUCCACGUACCAGCCUGGAUG**AAGCGAGCA**CGUCCAGGCUGGUAU
		GGCCGAGCGGCUGAAGGCACUCGUAGUG**AAGCAGGCA**CGCUACGAGUAGGUUGCC**CCAGAG**UC
	D1t	GGCAGCCUCCGUGGUUCGAAUCCACGUACCAGCCUGGAUG**AAGCCUCCA**CGUCCAGGCUGGUAU
		GGCCGAGCGGCUGAAGGCACUCGUAGUG**AAGCUCGCA**CGCUACGAGUAGGUUGCC**CCAGAG**UC
TS4	A1t'	GGCACCUCCGUGGUUCGAAUCCACGUACCAGCCUGGAUG**AAGUGGACA**CGUCCAGGCUGGUAUG
		GCCGAGCGGCUGAAGGCACUCGUAGUG**AAGGAGGCA**CGCUACGAGUAGGUGCC**CUCUGG**UC
	B1t'	GGCACCUCCGUGGUUCGAAUCCACGUACCAGCCUGGAUG**AAGCCUGCA**CGUCCAGGCUGGUAUG
		GCCGAGCGGCUGAAGGCACUCGUAGUG**AAGUCCAGA**CGCUACGAGUAGGUGCC**CUCUGG**UC
	C1t'	GGCACCUCCGUGGUUCGAAUCCACGUACCAGCCUGGAUG**AAGCGAGCA**CGUCCAGGCUGGUAUG
		GCCGAGCGGCUGAAGGCACUCGUAGUG**AAGCAGGCA**CGCUACGAGUAGGUGCC**CUCUGG**UC
	D1t'	GGCACCUCCGUGGUUCGAAUCCACGUACCAGCCUGGAUG**AAGCCUCCA**CGUCCAGGCUGGUAUG
		GCCGAGCGGCUGAAGGCACUCGUAGUG**AAGCUCGCA**CGCUACGAGUAGGUGCC**CUCUGG**UC

B. Supplementary Figures

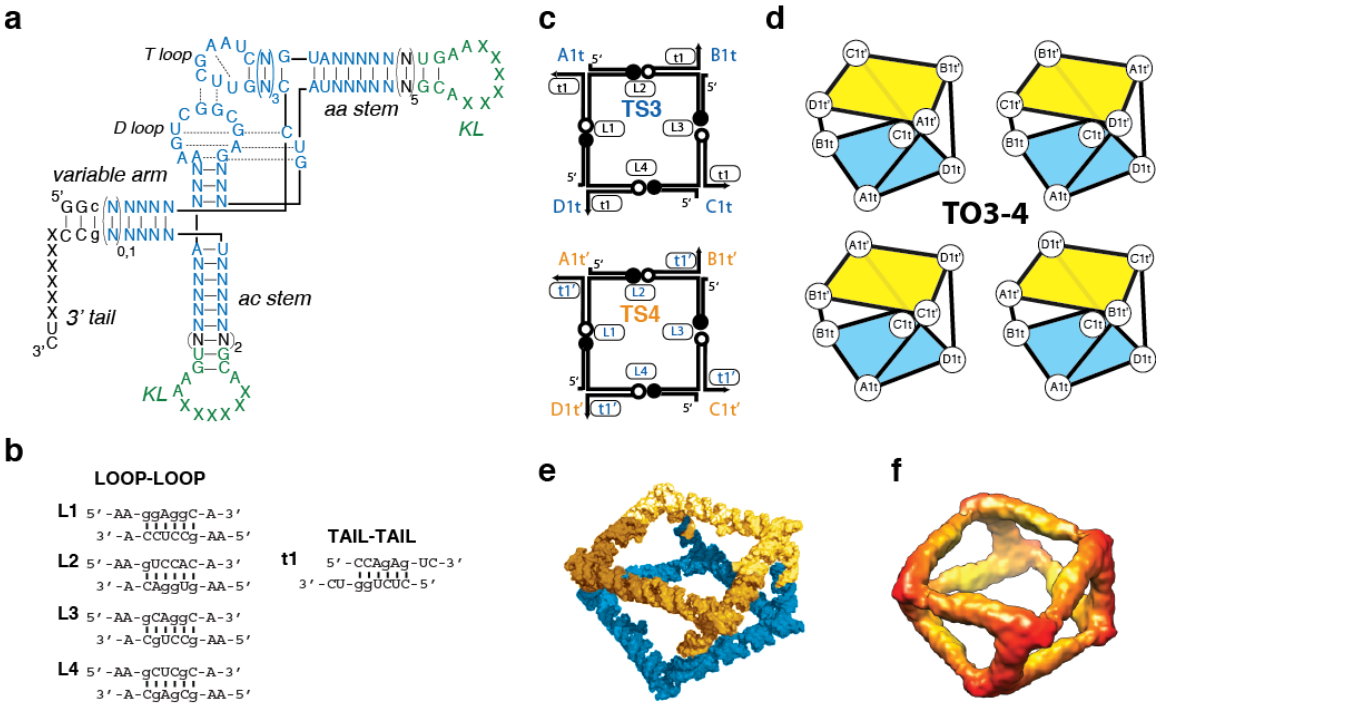

Figure S1: Design characteristics of the tRNA tectosquares and tRNA polyhedrons used in the study. **(a)** Generic secondary structure diagram for self-assembling tRNA units derived from the structure of Class II tRNA(Ser). The strand topology of the tRNA unit is designed so that the 5′ and 3′ ends are localized at the tip of the variable arm. Kissing-loops (KL) (in green) are inserted at the extremities of the ac and aa arms. Nucleotides in blue are those corresponding to the Class II tRNA(Ser) motif. N, any paired nucleotide; X, nucleotide involved in intermolecular KL or tail–tail base pairs. Dashed lines indicate tertiary interactions. The sequences corresponding to the tRNA units entering into the composition of TS3 and TS4 tectosquares are listed in Table S1. **(b)** Detail of the KL (loop-loop) and tail-tail interactions used to assemble the tRNA tectosquares TS3 and TS4 and the antiprism TO3-4. **(c)** Schematic of how the antiprism is assembled from TS3 and TS4. The KL and tail combinations for each unit are indicated. **(d)** Because TS3 has four identical 3' tails that are complementary to the four identical 3' tails of TS4, there are four different possible assembly combinations between TS3 and TS4. The four resulting conformers of TO3-4 are indicated. They should have the same overall three-dimensional shape. **(e)** Three-dimensional model adopted by the TO3-4 polyhedron. **(f)** Reconstructed cryo-EM 3D of the non-uniform antiprism TO1-2 (Severcan et al. (2010). TO3-4 adopts the same 3D structure as TO1-2.

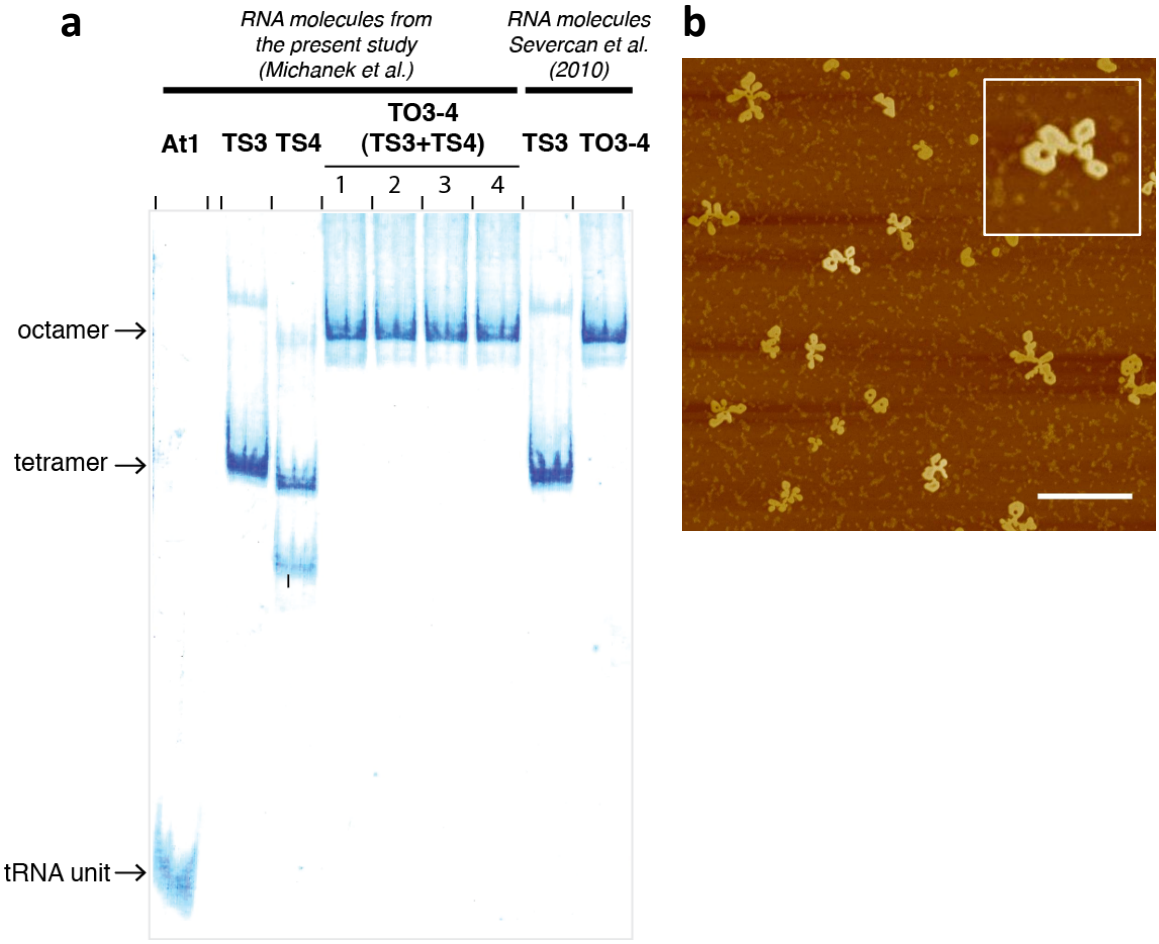

Figure S2. (a) Characterization of the tRNA square and anti-prism assemblies by native polyacrylamide gel electrophoresis at 15 mM $Mg(OAc)_2$ and 10°C. Lanes 1 to 4 for TO3-4 correspond to different RNA samples submitted to 0 min, 5 min, 15 min and 30 min of sonication respectively. RNA samples prepared as described in the Material and Methods were visualized by blue staining. Samples TS3 and TO3-4 on the right of the gel correspond to those prepared for the study published in Severcan et al (2010). TS3, TS4 and TO3-4 were extensively characterized by PAGE and temperature gradient gel electrophoresis (or TGGE) (Severcan et al (2010)). **(b)** AFM image of TS3 tectosquare on mica in air. The inset shows a close up of several squares. The scale bar is 1 µm.

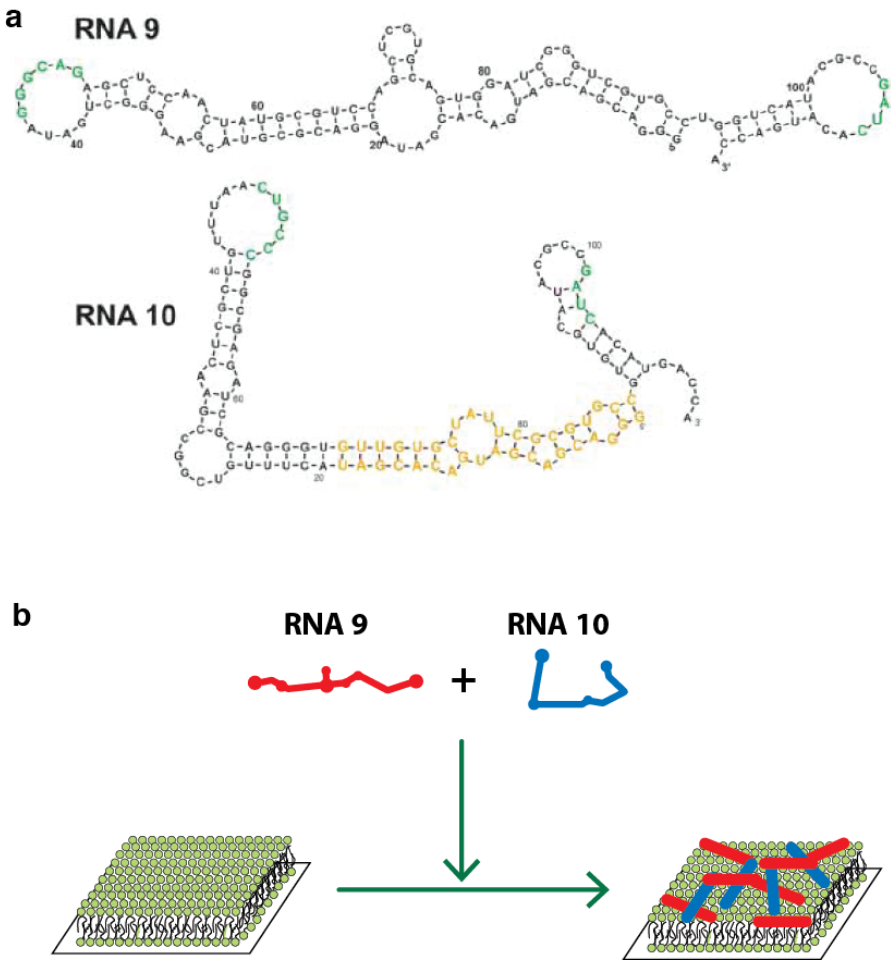

Figure S3: Secondary structures for the RNA-9 and RNA-10 molecules used in this study **(a)**. These molecules have previously been proposed to assemble through loop-loop interactions (regions indicated in green) to form RNA networks on lipid layers (Vlassov et al (2001)). According to Vlassov et al. (2001), the stoichiometry in the network is two RNA-9 molecules for one RNA-10. The diagrams are adapted from Janas and Yarus (2004). **(b)** According to our QCM data, the RNA molecules likely adsorb on the lipid surface without protruding much. The RNA network formed by RNA-9 and RNA-10 on lipid layers has been visualized by AFM by Janas and Yarus (2003). Their data suggests a rather disorganized RNA network.

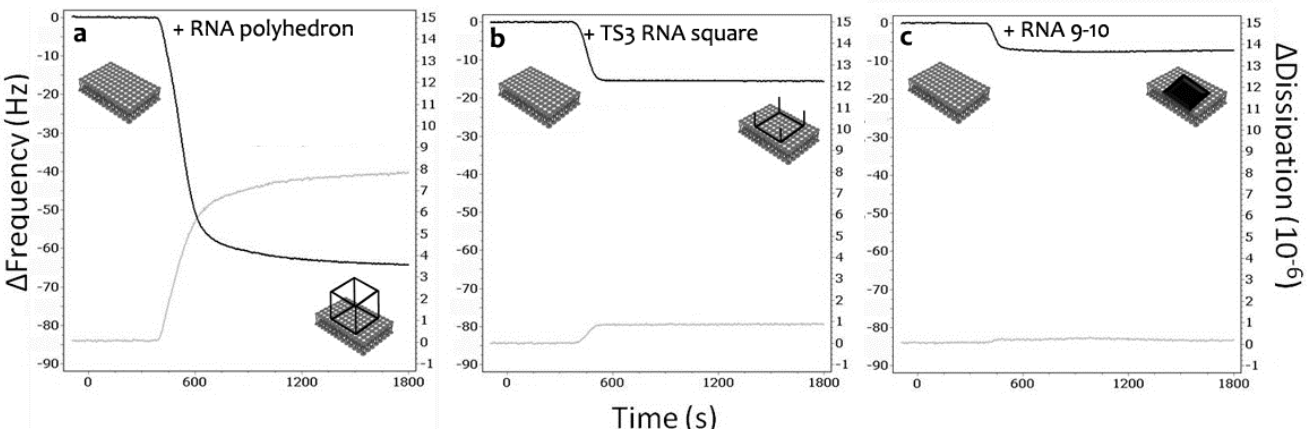

Figure S4: QCM-D data (overtone 7) for the adsorption of **(a)** RNA polyhedrons, **(b)** TS3 RNA tectosquares and **(c)** the complex of two oligonucleotides, $RNA_{9\text{-}10}$ to DOTAP bilayers. Both the frequency shift (black curves, left-hand axis) and the dissipation shift (grey curves, right-hand axis) are significantly larger for the adsorption of the TO3-4 RNA polyhedron compared to the adsorption of TS3. Adsorption of $RNA_{9\text{-}10}$ gives rise to even smaller change in frequency and no change in the dissipation. ΔF and ΔD values give measured differences relative to bare lipid bilayer.

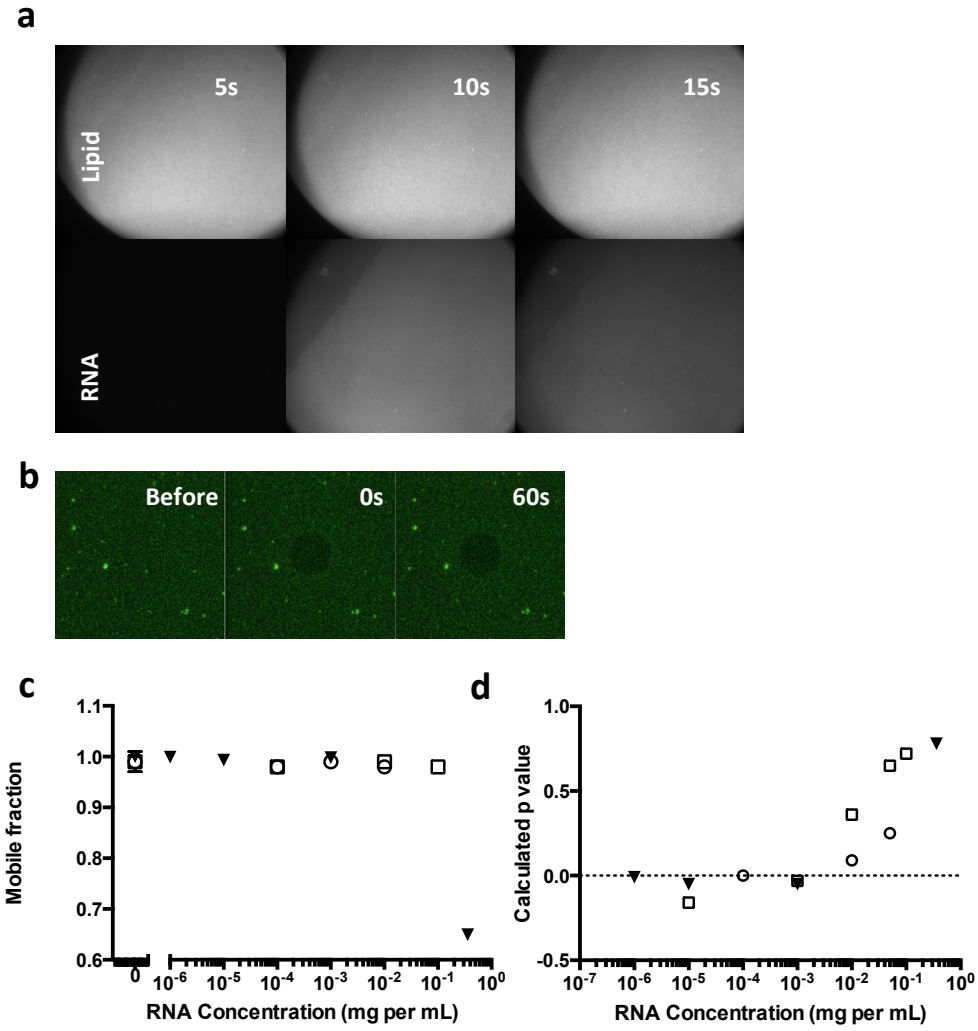

Figure S5: Representative TIRF images of time-course of adsorption of RNA polyhedron (0.001 mg mL^{-1}) labeled with GelStar probe (10X nominal concentration) on DOTAP with the fluorescence from the bilayer probe shown in the upper panel and the fluorescence from the adsorbing RNA label shown in the lower panel (**a**). Bleaching of RNA polyhedron (0.1 mg mL^{-1}) labeled with GelStar probe (10X nominal concentration) on DOTAP bilayers. Images (40 x 40 μm) of the RNA before, immediately and 60 s after bleaching are shown. **(b)**. The mobile fraction for DOTAP bilayers after exposure to increasing RNA polyhedron concentrations **(c)**. The calculated fraction (*p*) of the labeled DOTAP surface on which probe cannot move (**d**). The value of *p* was obtained as from equation 3 in the main text using the D value from the FRAP experiments performed on a scanning confocal microscope on bilayers of DOTAP labeled with NBD-DOTAP (open circles) and Rhodamine-PE (open squares), or a TIRF microscope on bilayers of DOTAP labeled with Rhodamine-PE (solid triangles). The diffusion coefficients of (negatively charged) Rh-PE in the neat DOTAP bilayers was measured to be 3.2 um^2/s from FRAP experiments using confocal microscope and 4.1 um^2/s from FRAP experiments using TIRF microscope. The difference can be explained by the use of different surface cleaning protocols and experimental methods. The diffusion coefficients of (positively charged) NBD-DOTAP in the neat DOTAP bilayers was measured to be 1.6 um^2/s from FRAP experiments using confocal microscope. The lower value of the measured diffusion coefficient can be explained by electrostatic attraction between the probe and the slightly oppositely charged glass surface.

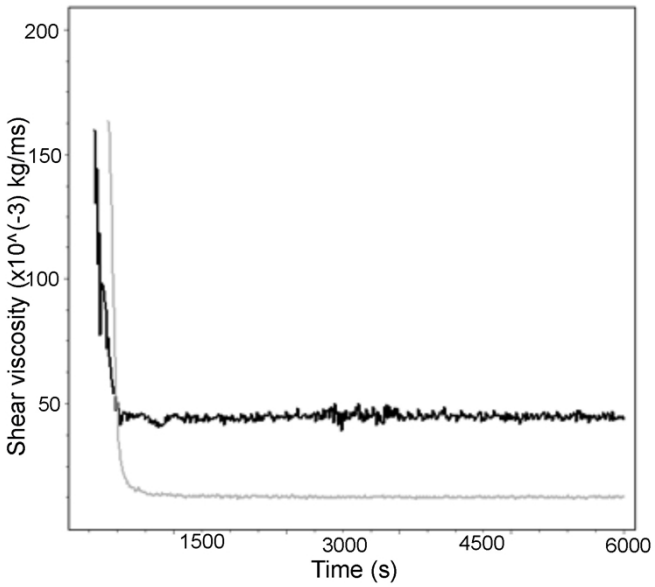

Figure S6: A correlation plot of change in shear viscosity as a function of time (on=7) for TS3 tectosquare (light grey curve) and TO3-4 polyhedron (black curve). A rapid decrase in shear is observed as the RNA assemblies are adsorbed to the bilayer (DOTAP) indicating that the adsorbed layer goes from compact to extended into the solution during the adsorption.

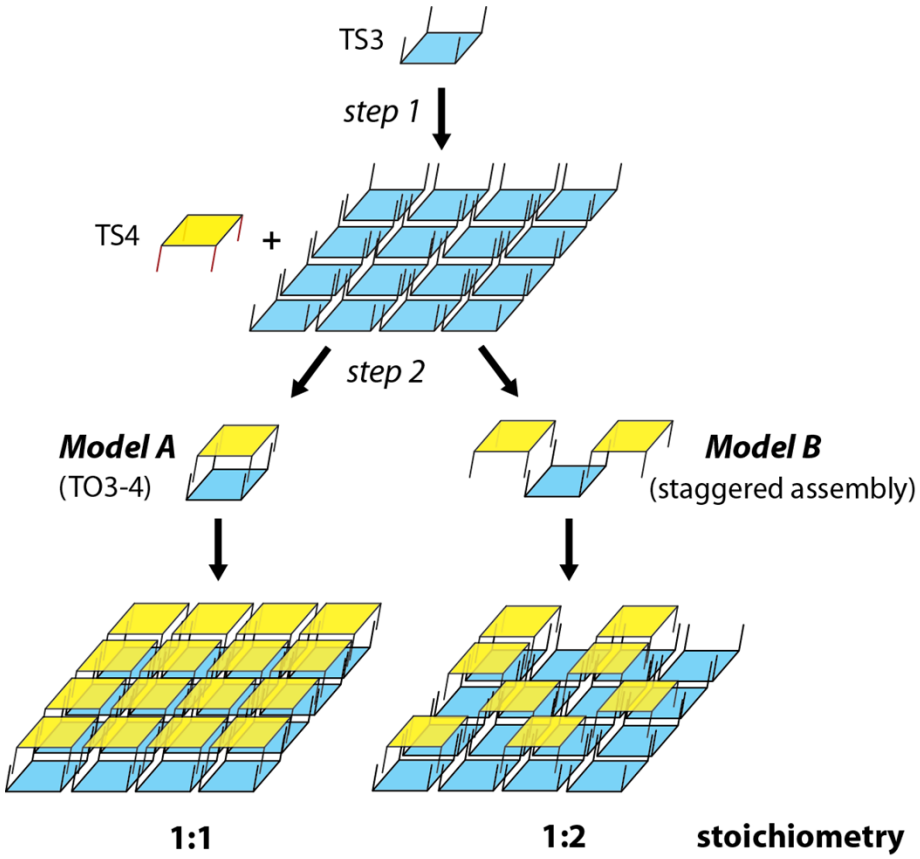

Figure S7: Models for the stoichiometry of TS in stepwise assembly on the lipid bilayer. ***Model A:*** 1:1 (TS4:TS3) stoichiometry can only be achieved when the assembly is compatible with the formation of TO3-4 RNA polyhedron. ***Model B:*** Staggered assembly, which can occur if assembly is not spatially and geometrically controlled by the RNA nanostructure, would lead to stoichiometric ratio as low as 1:2 for TS4:TS3. Experimental data indicate a ratio of approximately 1 (Figure 4c, ellipsometry data) that is compatible with model A, in which virtually all TS4 assemble with adsorbed TS3 to form TO3-4 polyhedrons.

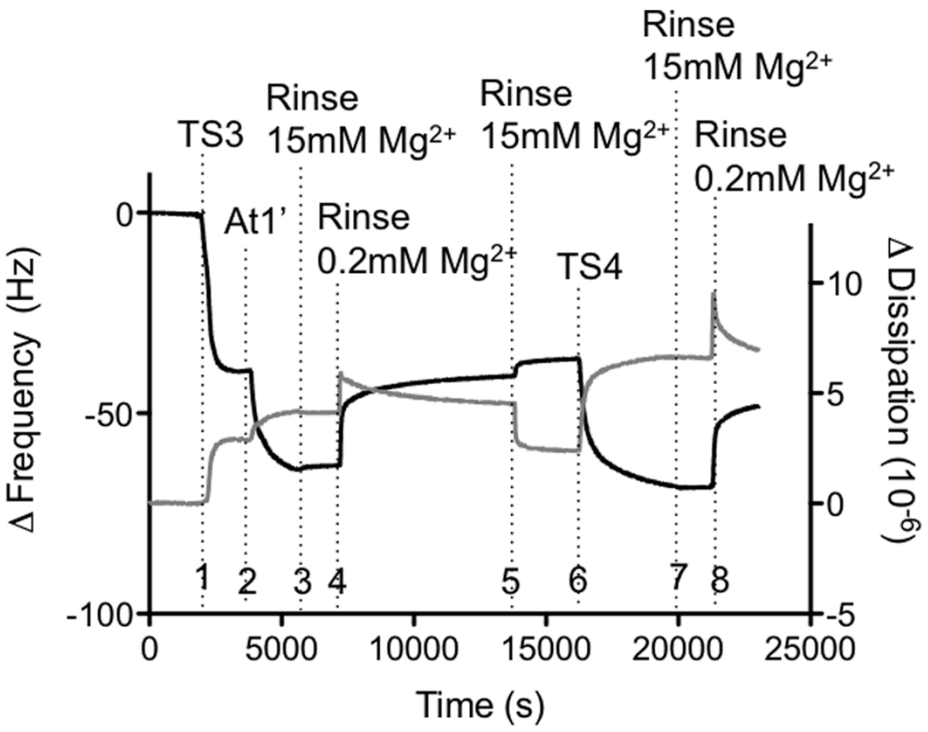

Figure S8: QCM frequency and dissipation data (overtone 7) for a sequential experiment in Figure 6a. (step 1): The TS3 tectosquare is adsorbed on a DOTAP bilayer. The large shift in ΔD implies extended surface structure. (step 2): After rinsing in buffer (15 mM Mg^{2+}), the A1t' tRNA units are added, which leads to a decrease inΔF and an increase in ΔD. This is interpreted as pairing of the A1t' tRNA tail region with the complementary single stranded tails of TS3. (step 3): Rinsing in buffer with 15 mM Mg^{2+} does not lead to desorption of any detectable change in surface structure. (step 4): Rinsing in buffer with 0.2 mM Mg^{2+}, on the other hand, lead to an increase in ΔF, which indicate desorption. A complication in the interpretation of these QCM-D data is that both ΔF and ΔD are affected by changing the buffer, which is here seen as a sudden and sharp increase in ΔD when the buffer solution is changed. Quantitative comparisons can therefore only be done between situations where the buffer is the same. In the present experiment, this is possible after (step 5) the subsequent change to the buffer with 15 mM Mg^{2+}. It is notable that the change in ΔF after the addition of A1t' almost equals the opposite change in ΔF when replacing the RNA solution for neat buffer in 2 steps, suggesting removal of the A1t' during rinsing. (step 6) The full TS4 tectosquare is then added, and the measured ΔF and ΔD are almost identical to the corresponding changes measured when TS4 tectosquare is added directly to the pre-adsorbed TS3 tectosquares without intermediate steps (compare Figure 5b). This imply that the tail regions on the pre-adsorbed TS3 tectosquare are again available for base pairing after the removal of the A1t' tRNA units. (step 7): Rinsing in buffer with 15 mM Mg^{2+} does not lead to desorption, while (step 8) rinsing in buffer with 0.2 mM Mg^{2+} leads partial desorption of the TS3 tectosquare, as implied from the measured increase in ΔF.

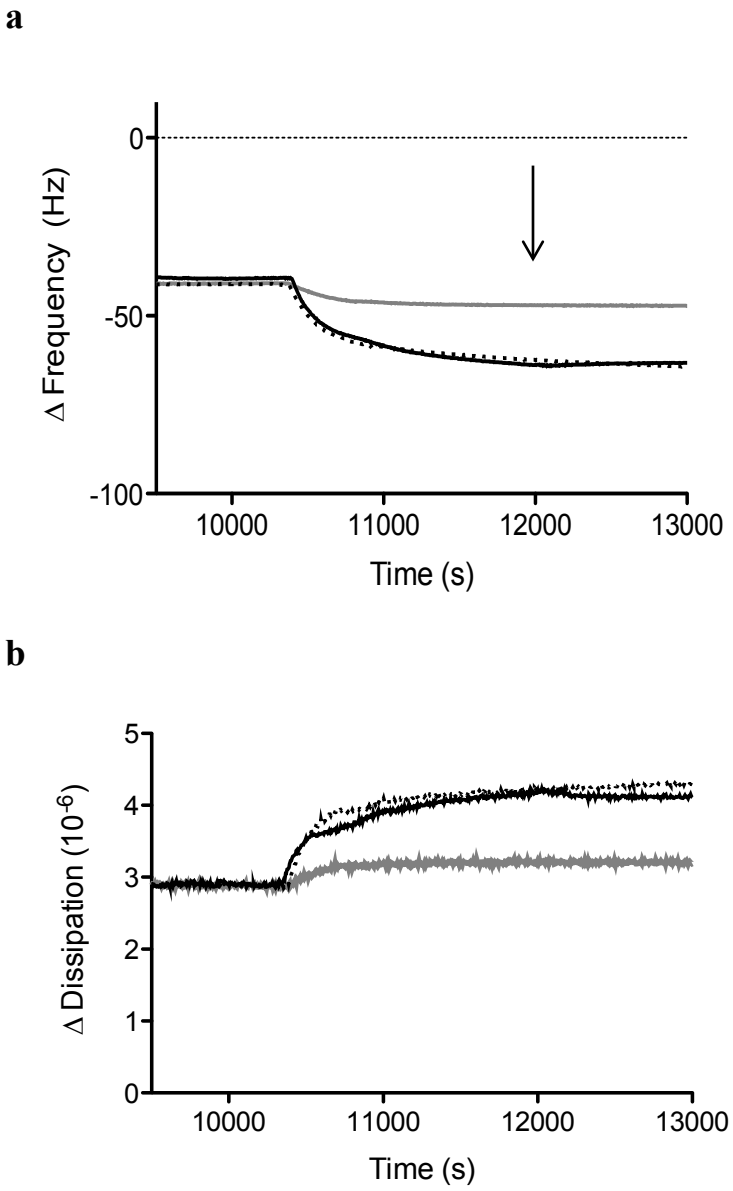

Figure S9: QCM-D frequency (**a**) and dissipation (**b**) data (overtone 7) for the addition of A1t' to TS3 tectosquare to a deposited DOTAP bilayer at different bulk concentrations: 2 μg/mL (Grey line), 10 μg/mL (Black solid line), and 20 μg/mL (Black dotted line). The data show that the bilayer is saturated already at bulk A1t' tRNA bulk concentration of 10 μg/mL, which is the same concentration as used in the experiment described in Figure 6a,b and Figure S4. Rinsing with buffer is shown with an arrow.

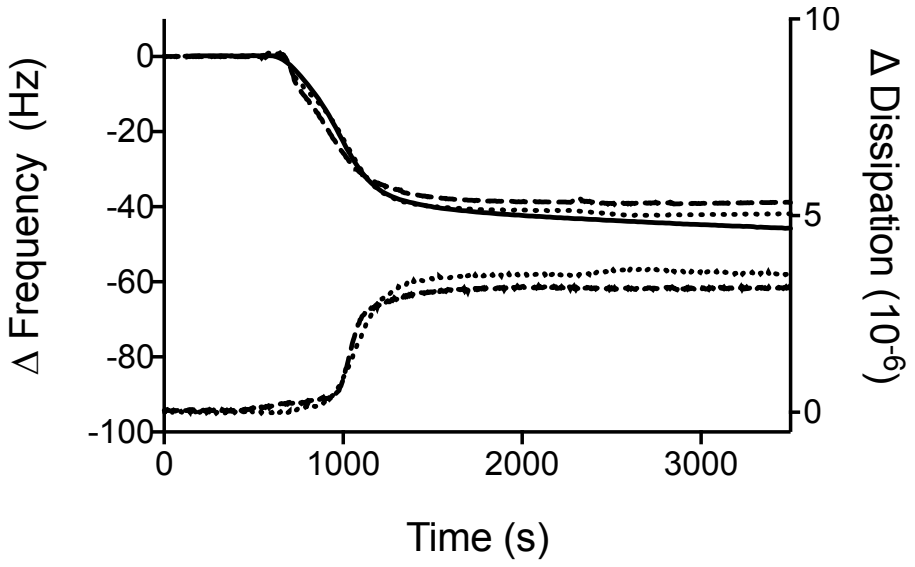

Figure S10: QCM-D frequency data (overtone 7) for three independent experiments showing the addition TS3 tectosquare (10 μg/mL) to a deposited DOTAP bilayer. Upper curves: ΔF (left axis), Lower curves: ΔD (left axis).

C. Additional references

Severcan, I.; Geary, C.; Chworos, A.; Voss, N.; Jacovetty, E.; Jaeger, L. *Nature Chemistry* **2010**, *2*, 772.
Vlassov, A.; Khvorova, A.; Yarus, M. *PNAS USA* **2001**, *98*, 7706.
Janas, T.; Yarus, M. *RNA* **2003**, *9*, 1353.
Janas, T.; Janas, T.; Yarus, M. *RNA* **2004**, *10*, 1541
Janas, T.; Janas, T.; Yarus, M. *Nucleic Acids Res.* **2006**, *34*, 2128.